Validation of the Exoplanet Kepler-21b using PAVO/CHARA Long-Baseline Interferometry

Daniel Huber^{1,2*}, Michael J. Ireland^{1,3,4}, Timothy R. Bedding¹, Steve B. Howell², Vicente Maestro¹, Antoine Mérand⁵, Peter G. Tuthill¹, Timothy R. White¹, Christopher D. Farrington⁶, P. J. Goldfinger⁶, Harold A. McAlister⁶, Gail H. Schaefer⁶, Judit Sturmann⁶, Laszlo Sturmann⁶,

Theo A. ten Brummelaar⁶, and Nils H. Turner⁶

- ¹Sydney Institute for Astronomy (SIfA), School of Physics, University of Sydney, NSW 2006, Australia
- ²NASA Ames Research Center, Moffett Field, CA 94035, USA
- ³Department of Physics and Astronomy, Macquarie University, NSW 2109, Australia
- 4 Australian Astronomical Observatory, PO Box 296, Epping, NSW 1710, Australia
- ⁵ European Southern Observatory, Alonso de Cordova 3107, Casilla 19001, Vitacura, Santiago 19, Chile
- ⁶ Center for High Angular Resolution Astronomy, Georgia State University, PO Box 3969, Atlanta, GA 30302, USA

Accepted -. Received -; in original form -

ABSTRACT

We present long-baseline interferometry of the Kepler exoplanet host star HD 179070 (Kepler-21) using the PAVO beam combiner at the CHARA Array. The visibility data are consistent with a single star and exclude stellar companions at separations $\sim 1\text{--}1000\,\mathrm{mas}~(\sim 0.1\text{--}113\,\mathrm{AU})$ and contrasts <3.5 magnitudes. This result supports the validation of the $1.6\,R_{\oplus}$ exoplanet Kepler-21b by Howell et al. (2012) and complements the constraints set by adaptive optics imaging, speckle interferometry, and radial velocity observations to rule out false-positives due to stellar companions. We conclude that long-baseline interferometry has strong potential to validate transiting extrasolar planets, particularly for future projects aimed at brighter stars and for host stars where radial velocity follow-up is not available.

Key words: stars: individual: HD 179070 – planets and satellites: individual: Kepler-21b – techniques: interferometric.

1 INTRODUCTION

The NASA Kepler Mission aims to find extrasolar planets in the habitable zones of solar-type stars through the detection of brightness dips as planets cross the stellar disc. While Kepler has been highly successful in finding exoplanet candidates, ground-based follow-up observations are important to confirm the detections. The most common astrophysical false positives for Kepler involve stellar companions that remain unresolved due to Kepler's large pixel size (~ 4 "). False positives can be divided into companions that are physically bound to the target star (hierarchical triple systems) and companions that are either in the foreground or the background of the target due to chance alignment (blends). In both cases, a transit-like shape can be mimicked by eclipses

of a stellar companion or transits of a planet around the secondary companion.

For large (Jupiter- and Neptune-sized) planets, candidates can often be confirmed using radial velocity observations, giving a direct estimate of the planet's mass (see, e.g., Borucki et al. 2010; Koch et al. 2010; Latham et al. 2010; Cochran et al. 2011), while transit timing variations can be used to confirm planets in multiple systems (see, e.g., Fabrycky et al. 2012; Ford et al. 2012; Steffen et al. 2012). For many super-Earths and Earth-sized planets, however, the Doppler signature is typically too small compared to the intrinsic stellar variability, and transit timing variations might not be detected. In these cases, candidates are validated by excluding as many false-positive scenarios as possible. The first stage in this process uses the Kepler data to detect signatures of stellar companions through photocenter shifts and the comparison of

^{*} NASA Postdoctoral Program Fellow, daniel.huber@nasa.gov

transit depths (see, e.g., Batalha et al. 2010; Bryson et al. 2010), followed by statistical modeling of potential blending scenarios (see, e.g., Torres et al. 2011; Fressin et al. 2011; Morton & Johnson 2011). These constraints are then combined with ground-based follow-up observations such as spectroscopy, speckle interferometry and adaptive optics imaging (see, e.g., Gautier et al. 2010; Howell et al. 2011). High-angular-resolution observations using long-baseline interferometry offer a powerful tool to complement these methods and extend the parameter range that can be excluded, particularly for close-in (both bound and unbound) companions.

Howell et al. (2012) recently reported the detection of Kepler-21b, a $1.6 R_{\oplus}$ planet in a 2.8 d orbit around the bright (V=8.3) F $\acute{6}$ IV star HD 179070. Extensive followup observations have been used to rule out a false positive detection in this system. Speckle interferometry rules out any unbound or bound stellar companions at separations > 0.2" ($\gtrsim 22.6 \,\mathrm{AU}$) for contrasts up to 5 mag, and at separations > 0.05" ($\gtrsim 5.6 \,\mathrm{AU}$) for contrasts up to 4 mag. Adaptive optics imaging revealed a $\sim 14.5\,\mathrm{mag}$ companion at a separation of 0.7" which, however, was found unable to mimick the observed transit shape due to its low mass. Radialvelocity time series were also obtained, and showed no significant variation over 85 days at a 5.6 m/s level. Putting all these constraints together, the only possibilities escaping direct detection are close-in bound companions within $\sim 4 \,\mathrm{mag}$ of HD 179070 in nearly face-on orbits (causing no detectable RV signature) with a similar radial velocity to the target star, and close-in blends within ~ 7 mag that may have escaped spectroscopic detection. Here, we present longbaseline interferometry observations to complement and extend the validation efforts by Howell et al. (2012).

2 OBSERVATIONS

We have observed HD 179070 as part of our interferometric follow-up campaign of Kepler stars using the PAVO (Precision Astronomical Visible Observations) beam combiner (Ireland et al. 2008) at the CHARA (Center for High Angular Resolution Astronomy) Array (ten Brummelaar et al. 2005). PAVO is a three-beam pupil-plane beam combiner optimized for high sensitivity and angular resolution, recording visibilities over a spectral bandpass of $\sim 650-800$ nm with a limiting magnitude in typical seeing conditions of $R \lesssim 8$ mag. Using baselines reaching up to 330 m, PAVO/CHARA is capable of resolving angular sizes down to ~ 0.3 mas. For more details on the instrument and data reduction, we refer to Ireland et al. (2008).

HD 179070 was observed on 2 July 2011 in two-telescope mode using the S1-W1 (278 m) baseline in excellent seeing conditions. Two scans were obtained, which were interleaved with observations of three different calibrator stars. Using various catalogs available in the literature, calibrators are typically chosen to be single field stars in close vicinity ($< 10^{\circ}$) to the target star. Table 1 lists the spectral types, photometric properties, and expected sizes of all stars in this study. The predicted sizes were calculated using the (V-K) relation given by Kervella et al. (2004). V magnitudes have been extracted from the Tycho catalog (Perryman & ESA 1997) and transformed into the Johnson

Table 1. Spectral types, photometry and expected angular sizes of stars in this study. Brackets indicate the last two digits of the 1σ uncertainties.

HD	Sp.T.	V	K	θ_{V-K} (mas)
179070	F6IV	8.262(11)	6.945(18)	0.169(09)
$ \begin{array}{r} 174260 \\ 178591^1 \\ 183204 \end{array} $	B8V B5V A0V	7.323(05) 7.130(57) 7.425(07)	7.465(18) 7.191(24) 7.386(21)	0.103(05) 0.119(06) 0.110(06)

 $^{^1}$ HD 178591 is an ellipsoidal variable with an amplitude of $\sim 0.05\,\mathrm{mag}.$

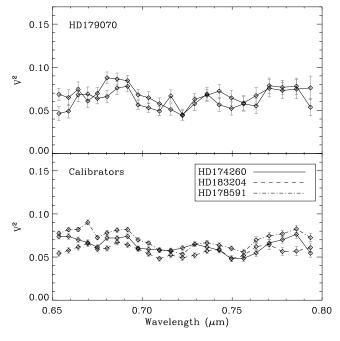


Figure 1. Raw visibility versus wavelength for the target HD 179070 (top panel) and the calibrator stars (bottom panel).

system using the calibration of Bessell (2000). K magnitudes have been obtained from the 2MASS catalog (Cutri et al. 2003; Skrutskie et al. 2006). We have tested the photometry for reddening by comparing the observed (B-V) colors with a list of intrinsic colors as a function of spectral type given by Schmidt-Kaler (1982). The observed colors have been found to be compatible with the spectral types for all stars except for the calibrator HD 178591, which is classified as an ellipsoidal variable by Hipparcos. We have accounted for this by adding a systematic uncertainty corresponding to the observed variability amplitude ($\sim 0.05 \,\mathrm{mag}$) to the statistical photometric uncertainty in the V band. Note that the potential companion of HD 178591 can be expected to have a negligible influence on the interferometric measurements. The final uncertainties for the predicted angular diameters were calculated by adding a conservative 5% calibration uncertainty in quadrature to the photometric uncertainty.

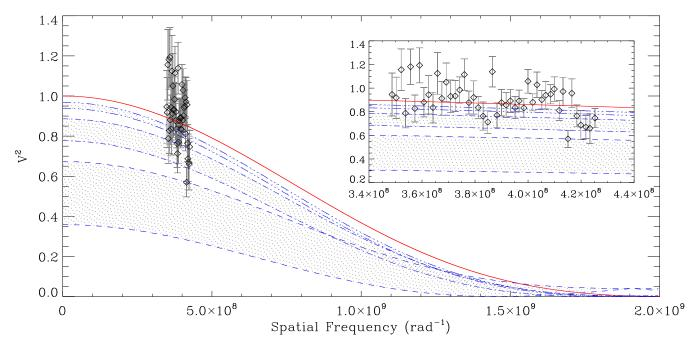


Figure 2. Calibrated squared visibility versus spatial frequency for HD 179070. The red solid line shows the best fitting single disc model with a diameter of $\theta_{\rm LD} = 0.13 \pm 0.02\,{\rm mas}$. The areas marked by blue dashed, dashed-dotted and dashed-triple-dotted lines show the range of minimum squared visibilities expected for companions $> 1\,{\rm mas}$ with contrasts of 1.5, 3 and 4.5 magnitudes, respectively. The inset shows a close-up of the data.

3 RESULTS AND DISCUSSION

Figure 1 shows the raw squared visibility measurements across the PAVO passband for the target and the calibrators. As expected from their predicted sizes, the visibility levels of the calibrators are very similar. Note that the raw measurements are considerably lower than the expected visibilities (~ 0.9) due to atmospheric turbulence and optical aberrations. HD 179070 remains practically unresolved in our observations, with raw visibilities at very similar levels to the calibrator stars, and no significant visibility change as a function of wavelength. More importantly, the similarity between target and calibrator scans shows that the visibility curve of HD 179070 is consistent with a single star. For any companion for which the interference patterns (fringe packets) of the two stars overlap in delay space, a periodic visibility modulation would be observed, while any incoherent flux from companions at larger separations would cause a drop in the observed visibility (see, e.g., Monnier 2003; ten Brummelaar 2007). The interferometric field of view for each case depends on the coherence length and the projected baseline (ten Brummelaar 1995), and for our observations corresponds to <30 mas and 30–1000 mas, respectively.

To illustrate this more clearly, Figure 2 shows the calibrated squared visibility data of HD 179070 as a function of spatial frequency. Visibilities were calibrated by dividing the calibrator data by the predicted sizes to obtain a system visibility, which was then used to correct the target visibility. We then fitted the limb-darkened disc model given by Hanbury Brown et al. (1974) to the data using the method described by Derekas et al. (2011). We used a linear limb-darkening coefficient for the R-band of $\mu_R=0.5197$, derived from the closest matching grid point of Claret & Bloemen

(2011) to the stellar parameters presented by Howell et al. (2012). The red line in Figure 2 shows the best-fitting singledisc model, yielding a diameter of $\theta_{\rm LD} = 0.13 \pm 0.02$ mas with a reduced $\chi^2 = 1.4$. This diameter agrees with the diameter of 0.15 ± 0.01 mas constrained from the asteroseismic radius $(R/R_{\odot}) = 1.86 \pm 0.02$, Howell et al. 2012) and Hipparcos parallax ($\pi = 8.86 \pm 0.58$ mas, van Leeuwen 2007). The areas marked by blue dashed, dashed-dotted, and dashed-tripledotted lines illustrate the minimum squared visibilities expected for a stellar companion with a contrast of 1.5, 3 and 4.5 magnitudes compared to HD 179070. Deep minima correspond to close-in companions (1–30 mas) which will show a periodic variation across the PAVO passband, while shallower minima correspond to wide companions (> 30 mas), for which the variation is unresolved within the spectral resolution of PAVO and hence an overall drop in visibility would be observed. Figure 2 suggests that the PAVO observations rule out any stellar companions at contrasts of $\lesssim 3$ magnitudes. Note that for stellar companions at even closer separations ($\lesssim 0.1 \,\mathrm{AU}$), the PAVO data would solely exclude companions along the baseline vector at the time of observation, which in this case spans only one epoch. We also note that the faint $\sim 14.5 \,\mathrm{mag}$ companion at ~ 0.7 " detected by Howell et al. (2012) has negligible influence on our measurements.

To establish the magnitude limit more quantitatively, we performed 10^5 simulations as follows. For each iteration, we used the spatial frequencies of our observations to generate a synthetic binary model consisting of a primary with the expected size of HD 179070 and an unresolved secondary, with a separation and contrast drawn from uniform distributions between 1–50 mas and 1–6 mag, respectively. We then added white noise to each data point with a standard devi-

ation corresponding to our estimated relative measurement uncertainties. For each simulated dataset, we then fitted a binary model to the data and compared the χ^2 value to the one calculated from a single disc model with the expected size of HD 179070. The simulations showed that in > 99%of all cases, the binary model yielded a significantly (> 3σ) better fit for contrasts below 3.6 magnitudes. This limit has been found to be only weakly dependent on the separation, dropping to $\sim 3.4 \,\mathrm{mag}$ for wide (50–1000 mas) binaries. To confirm the limit, we performed a Bayesian model comparison by calculating the odds ratio between both models. Equal prior probability of each model was assumed (hence simplifying the problem to the calculation of the Bayes factor). The marginal likelihood (evidence) for each model was calculated using Nested Sampling (Skilling 2004). We assumed a Gaussian prior probability for the primary diameter, and a uniform prior for the separation and contrast of the binary model. Due to computational reasons the calculation was performed for 150 simulations and restricted to a smaller range of close-in (1–10 mas) companions. The computed Bayes factors consistently favored the binary model over the single star model for contrasts < 3.5 mag. As expected, this value is more conservative than the limit inferred from the likelihood ratio, since the Bayesian model comparison penalizes the binary model for its added complexity. Based on these results, we conclude that our data would have revealed a stellar companion at separations ~ 1 - $1000 \,\mathrm{mas} \,(\sim 0.1 - 113 \,\mathrm{AU})$ and contrasts $< 3.5 \,\mathrm{magnitudes}$.

We note that the above simulations assume that our measurement uncertainties are well characterized. Previous PAVO observations of the same star over multiple nights showed that night-to-night variations in V^2 are at the 2–3% level (Huber et al. 2012, in preparation), while the ~ 5 % uncertainties in the calibrator sizes (see Table 1) translate to a 1% uncertainty in V^2 (van Belle & van Belle 2005). Both these contributions are considerably smaller than our measurement uncertainties (estimated from the scatter of individual data frames integrated over each scan), which are on average 13%. Combined with the low reduced χ^2 of our fit, we therefore argue that our measurement uncertainties are a good estimate of the total uncertainty in our data.

The results presented here complement and extend the constraints set by Howell et al. (2012). For the case of unbound companions, the PAVO limit of $< 3.5 \,\mathrm{mag}$ covers only a small range of the possible false-positive scenarios, which extend down to <7 mag. Additionally, Howell et al. (2012) demonstrated that the probability of a chance alignment of a star able to reproduce the transit shape at such close separations is very small. Hence, the added information from PAVO for unbound companions is negligible. For the case of bound companions, Figure 3 illustrates the constraints from PAVO and speckle interferometry on the mass and separation of a possible secondary. Magnitude limits were converted into mass limits by interpolating a 3 Gyr solarmetallicity isochrone by Baraffe et al. (1998), which roughly matches the age of HD 179070 as determined by the asteroseismic analysis in Howell et al. (2012). Additionally, we plot the 3- σ detection limit from radial velocity follow-up for different inclinations, assuming a circular orbit for the hypothetical companion and a simple linear velocity change with time. The diagram shows that PAVO rules out face-on orbits for bound companions at separations $\lesssim 5.6 \,\mathrm{AU}$, which

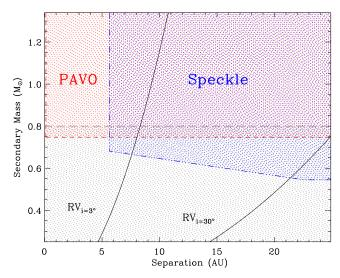


Figure 3. Constraints on the mass and separation of a secondary companion to HD 179070 from PAVO (red dashed line) and Speckle interferometry (blue dashed-triple-dotted line). Magnitude limits have been converted into secondary masses by interpolating a 3 Gyr solar-metallicity isochrone by Baraffe et al. (1998). Black solid lines show the limit from RV follow-up for different inclinations, with any companion to the left of the lines being detectable with an average radial velocity signal $> 16.8 \, \text{m/s}$ ($> 3\,\sigma$) over a timespan of 85 days. Note that any false-positive detection for secondaries with masses $\lesssim 0.8\,M_{\odot}$ (marked by a long-dashed line) can be ruled out from the observed Kepler transit shape (see Howell et al. 2012).

could previously not be excluded, and confirms the constraints set by complementary follow-up methods. Since a planet transiting a secondary with a mass lower than $0.8\,M_{\odot}$ can be excluded from the Kepler transit shape (Howell et al. 2012), the combined constraints virtually rule out any possible false-positive scenario involving a gravitationally bound companion around HD 179070.

4 CONCLUSIONS

We have presented high-angular-resolution observations of the exoplanet host star HD 179070 (Kepler-21) using the PAVO beam combiner at the CHARA Array. Our data clearly rule out stellar companions at separations between $\sim 1\text{--}1000~\mathrm{mas}~(\sim 0.1\text{--}113~\mathrm{AU})$ with contrasts of $<3.5~\mathrm{magnitudes}$. This complements and extends the validation efforts by Howell et al. (2012), and supports the conclusion that the detected transit is due to a $1.6~R_{\oplus}$ extrasolar planet in an orbit around HD 179070.

The results shown here demonstrate the potential of PAVO/CHARA to validate transiting exoplanet candidates, and complement the existing efforts using long-baseline interferometry to characterize exoplanet host stars (see, e.g., Baines et al. 2009; van Belle & von Braun 2009; von Braun et al. 2011). Using a recent compilation of detected exoplanets in the NASA Exoplanet Archive¹, we estimate about half a dozen host stars with transiting exoplan-

http://exoplanetarchive.ipac.caltech.edu/index.html

ets to be accessible to observations with PAVO/CHARA. Furthermore, there will be a considerable overlap with the target sample of the planned Transiting Exoplanet Survey Satellite (TESS, Ricker et al. 2009), which is aimed at finding planets around nearby (V < 12) stars. While the contribution of PAVO to the validation effort of Kepler-21b is relatively modest, it can be expected that long-baseline interferometry will play a significant role in validating transiting extrasolar planets, in particular for future missions aimed at bright stars and for cases where precise radial-velocity follow-up may not be available.

ACKNOWLEDGMENTS

DH, TRB and VM acknowledge support from the Access to Major Research Facilities Program, administered by the Australian Nuclear Science and Technology Organisation (ANSTO). DH is supported by an appointment to the NASA Postdoctoral Program at Ames Research Center, administered by Oak Ridge Associated Universities through a contract with NASA. The CHARA Array is funded by the National Science Foundation through NSF grant AST-0606958, by Georgia State University through the College of Arts and Sciences, and by the W.M. Keck Foundation. This publication makes use of data products from the Two Micron All Sky Survey, which is a joint project of the University of Massachusetts and the Infrared Processing and Analysis Center/California Institute of Technology, funded by the National Aeronautics and Space Administration and the National Science Foundation. This research has made use of the NASA Exoplanet Archive, which is operated by the California Institute of Technology, under contract with the National Aeronautics and Space Administration under the Exoplanet Exploration Program.

REFERENCES

Baines E. K., McAlister H. A., ten Brummelaar T. A., Sturmann J., Sturmann L., Turner N. H., Ridgway S. T., 2009, ApJ, 701, 154

Baraffe I., Chabrier G., Allard F., Hauschildt P. H., 1998, A&A, 337, 403

Batalha N. M. et al., 2010, ApJ, 713, L103

Bessell M. S., 2000, PASP, 112, 961

Borucki W. J. et al., 2010, Science, 327, 977

Bryson S. T. et al., 2010, ApJ, 713, L97

Claret A., Bloemen S., 2011, A&A, 529, A75

Cochran W. D. et al., 2011, ApJS, 197, 7

Cutri R. M. et al., 2003, 2MASS All Sky Catalog of point sources., Cutri, R. M., Skrutskie, M. F., van Dyk, S., Beichman, C. A., Carpenter, J. M., Chester, T., Cambresy, L., Evans, T., Fowler, J., Gizis, J., Howard, E., Huchra, J., Jarrett, T., Kopan, E. L., Kirkpatrick, J. D., Light, R. M., Marsh, K. A., McCallon, H., Schneider, S., Stiening, R., Sykes, M., Weinberg, M., Wheaton, W. A., Wheelock, S., & Zacarias, N., ed.

Derekas A. et al., 2011, Science, 332, 216

Fabrycky D. C. et al., 2012, ApJ, in press (arXiv:1201.5415)

Ford E. B. et al., 2012, ApJ, in press (arXiv:1201.5409)

Fressin F. et al., 2011, ApJS, 197, 5

Gautier, III T. N. et al., 2010, arXiv:1001.0352

Hanbury Brown R., Davis J., Lake R. J. W., Thompson
 R. J., 1974, MNRAS, 167, 475

Howell S. B., Everett M. E., Sherry W., Horch E., Ciardi D. R., 2011, AJ, 142, 19

Howell S. B. et al., 2012, ApJ, 746, 123

Ireland M. J. et al., 2008, in Presented at the Society of Photo-Optical Instrumentation Engineers (SPIE) Conference, Vol. 7013, Society of Photo-Optical Instrumentation Engineers (SPIE) Conference Series

Kervella P., Thévenin F., Di Folco E., Ségransan D., 2004, A&A, 426, 297

Koch D. G. et al., 2010, ApJ, 713, L131

Latham D. W. et al., 2010, ApJ, 713, L140

Monnier J. D., 2003, Reports on Progress in Physics, 66, 789

Morton T. D., Johnson J. A., 2011, ApJ, 738, 170

Perryman M. A. C., ESA, eds., 1997, ESA Special Publication, Vol. 1200, The HIPPARCOS and TYCHO catalogues. Astrometric and photometric star catalogues derived from the ESA HIPPARCOS Space Astrometry Mission

Ricker G. R. et al., 2009, in Bulletin of the American Astronomical Society, Vol. 41, American Astronomical Society Meeting Abstracts 213, p. 403.01

Schmidt-Kaler T., 1982, Stars and Star Clusters, Landolt-Börnstein, Group VI, Vol. 2b Springer. Springer

Skilling J., 2004, in American Institute of Physics Conference Series, Vol. 735, American Institute of Physics Conference Series, R. Fischer, R. Preuss, & U. V. Toussaint, ed., pp. 395–405

Skrutskie M. F. et al., 2006, AJ, 131, 1163

Steffen J. H. et al., 2012, MNRAS, in press (arXiv:1201.5412)

ten Brummelaar T. A., 1995, Appl. Opt., 34, 2214

ten Brummelaar T. A., 2007, in IAU Symposium, Vol. 240, IAU Symposium, W. I. Hartkopf, E. F. Guinan, & P. Harmanec, ed., pp. 178–187

ten Brummelaar T. A. et al., 2005, ApJ, 628, 453

Torres G. et al., 2011, ApJ, 727, 24

van Belle G. T., van Belle G., 2005, PASP, 117, 1263

van Belle G. T., von Braun K., 2009, ApJ, 694, 1085

van Leeuwen F., 2007, A&A, 474, 653

von Braun K. et al., 2011, ApJ, 729, L26